

## Fidelity approach to the Hubbard model

L. Campos Venuti,<sup>1</sup> M. Cozzini,<sup>1,2</sup> P. Buonsante,<sup>3,2</sup> F. Massel,<sup>2</sup> N. Bray-Ali,<sup>4</sup> and P. Zanardi<sup>4,1</sup>

<sup>1</sup>*ISI Foundation for Scientific Interchange, Villa Gualino, Viale Settimio Severo 65, I-10133 Torino, Italy*

<sup>2</sup>*Dipartimento di Fisica, Politecnico di Torino, Corso Duca degli Abruzzi 24, I-10129 Torino, Italy*

<sup>3</sup>*CNISM, Unità di Ricerca Torino Politecnico, Corso Duca degli Abruzzi 24, I-10129 Torino, Italy*

<sup>4</sup>*Department of Physics and Astronomy, University of Southern California, Los Angeles, California 90089-0484, USA*

(Received 16 January 2008; published 9 September 2008)

We use the fidelity approach to quantum critical points to study the zero-temperature phase diagram of the one-dimensional Hubbard model. Using a variety of analytical and numerical techniques, we analyze the fidelity metric in various regions of the phase diagram with particular care to the critical points. Specifically we show that close to the Mott transition, taking place at on-site repulsion  $U=0$  and electron density  $n=1$ , the fidelity metric satisfies an hyperscaling form which we calculate. This implies that in general, as one approaches the critical point  $U=0$ ,  $n=1$ , the fidelity metric tends to a limit which depends on the path of approach. At half-filling, the fidelity metric is expected to diverge as  $U^{-4}$  when  $U$  is sent to zero.

DOI: [10.1103/PhysRevB.78.115410](https://doi.org/10.1103/PhysRevB.78.115410)

PACS number(s): 64.60.-i, 03.65.Ud, 05.70.Jk, 05.45.Mt

### I. INTRODUCTION

Recently a characterization of phase transitions has been advocated.<sup>1</sup> This is the so-called fidelity approach to critical phenomena<sup>2-16</sup> that relies solely on the state of the system and does not require the knowledge of the model Hamiltonian and its symmetry-breaking mechanism. Two states of the system at nearby points in parameter space are compared by computing their overlap (the fidelity). Since quantum phase transitions are major changes in the structure of the ground state, it is natural to expect that when one crosses a transition point the fidelity will drop abruptly. To make the analysis more quantitative one considers the second derivative of the fidelity with respect to the displacement in parameter space. Remarkably this second derivative, more in general the Hessian matrix, defines a metric tensor (the fidelity metric hereafter) in the space of pure states.<sup>16</sup> A superextensive scaling of the fidelity metric corresponds to the intuitive idea of a fidelity drop. Indeed, it was shown in Ref. 17 that at regular points the fidelity metric scales extensively with the system size, and a superextensive behavior implies criticality. However the converse is not true in general; in order to observe a divergence in the fidelity metric a sufficiently relevant perturbation (in the renormalization-group sense) is needed.<sup>17</sup> Loosely speaking the more relevant the operator the stronger the divergence of the fidelity metric. The Berezinskii-Kosterlitz-Thouless (BKT) transition is peculiar in this respect as it is driven by a marginally relevant perturbation, i.e., with the smallest possible scaling dimension capable of driving a transition. This gives rise to an infinite order transition and as such the BKT does not rigorously fit in the simple scaling argument given in.<sup>17</sup>

Surprisingly, contrary to the naïve expectation, Yang<sup>15</sup> showed that in the particular instance of BKT transition provided by the spin-1/2 XXZ model, the fidelity metric diverges algebraically as a function of the anisotropy. This is an appealing feature since observing a singularity at a BKT transition is generally a difficult task.<sup>18</sup>

In this paper we analyzed, with a variety of analytical and numerical techniques, the one-dimensional (1D) Hubbard

model primarily aiming at assessing the power and limitations of the fidelity approach for infinite order Quantum Phase Transition (QPT) ( $n=1$ ,  $U \rightarrow 0$ ). We believe it is useful to list here the main accomplishment of our analysis. (i) An exact calculation, on the free-gas line  $U=0$ , shows that the fidelity metric  $g$  presents a cusp at half-filling and a  $1/n$  divergence at low density  $n$ , respectively. (ii) Using bosonization techniques, we observe a divergence of the form  $g \sim n^{-2}$  in the regime  $U \ll n$  when  $n \rightarrow 0$ . (iii) Resorting to Bethe-Ansatz we are able to interpolate between the regime where the Luttinger liquid (LL) parameter  $K$  approaches the BKT value of  $1/2$  and that where  $K \rightarrow 1$ , which describes the free-Dirac point. We show that the fidelity metric satisfies an hyperscaling equation which can also be extended to finite sizes. (iv) We calculate the hyperscaling function in the thermodynamic limit by solving Bethe-Ansatz integral equations while at half-filling by resorting to exact diagonalization. As a consequence, when approaching the transition point  $U=0$ ,  $n=1$ , the fidelity metric tends to a limit which depends on the path of approach. On the particular path  $U \rightarrow 0$ ,  $n=1$ , an algebraic divergence of the form  $g \sim U^{-4}$  is expected on the basis of numerical results.

In the 1D Hubbard model the BKT transition<sup>19</sup> occurs exactly at half-filling as soon as the on-site interaction  $U$  is switched on, inducing a gap in the charge excitation spectrum. Away from half-filling instead all modes are gapless for any  $U$  and the system is a Luttinger liquid. Since at half-filling the only gapless point is at  $U=0$ , the kind of BKT transition offered by the Hubbard model is different from that featured by the XXZ model. In that case one continuously arrives at the transition point from a gapless phase by tuning the anisotropy parameter. This difference, in turn, makes more difficult the analysis of the fidelity metric in the Hubbard model.

### II. PRELIMINARIES

The one-dimensional Hubbard model is given by

$$H = - \sum_{i,\sigma} (c_{i,\sigma}^\dagger c_{i+1,\sigma} + \text{H.c.}) + \sum_i n_{i,\uparrow} n_{i,\downarrow} - \mu \sum_i n_i, \quad (1)$$

where  $n_{i,\sigma} = c_{i,\sigma}^\dagger c_{i,\sigma}$  and  $n_i = n_{i,\uparrow} + n_{i,\downarrow}$  and we will be concerned with the repulsive/free-gas case when  $U \geq 0$ . Due to the symmetries of the model<sup>20</sup> it is sufficient to limit the analysis to filling smaller or equal to one half, i.e.,  $n \equiv \langle n_i \rangle \leq 1$ . It is well known<sup>21,22</sup> that for  $n < 1$  the model is in the Luttinger liquid universality class for any value of the interaction  $U$ . Spin and charge degrees of freedom separate and their respective excitations travel at distinct velocities  $v_s$  and  $v_c$ . Both charge and spin modes are therefore gapless. Exactly at half-filling ( $n=1$ ) the system becomes an insulator and develops a charge gap  $\Delta E_c = \mu_+ - \mu_- = E(N+1) - 2E(N) + E(N-1)$ , where  $E(N)$  is the ground-state energy with  $N$  particles. The gap opens up exponentially slow from  $U=0$ , and the point  $U=0, n=1$  is a transition of BKT type.<sup>23</sup> The length scale  $\xi = 2v_c / \Delta E_c$  describes the size of soliton-antisoliton pairs in the insulator. As we approach the critical point at  $U=0, n=1$ , these pairs unbind and proliferate, allowing the system to conduct.

In the fidelity approach one is interested in the overlap between ground states at neighboring points of the coupling constants (say, a vector  $\lambda$ ):  $F(\lambda) = |\langle \psi(\lambda) | \psi(\lambda + d\lambda) \rangle|$ . Remarkably, the second-order term in the expansion of the fidelity defines a metric in the space of (pure) states,

$$F(\lambda) = 1 - \frac{1}{2} G_{\mu,\nu} d\lambda^\mu d\lambda^\nu + O(d\lambda^3),$$

where

$$G_{\mu,\nu} = \text{Re}[\langle \partial_\mu \psi_0 | \partial_\nu \psi_0 \rangle - \langle \partial_\mu \psi_0 | \psi_0 \rangle \langle \psi_0 | \partial_\nu \psi_0 \rangle],$$

and  $\psi_0 = \psi(\lambda)$  and  $\partial_\mu = \partial / \partial \lambda^\mu$ . Actually, at regular points  $\lambda$  of the phase diagram,  $G_{\mu,\nu}$  is an extensive quantity<sup>17</sup> so that it is useful to define the related intensive metric tensor  $g_{\mu,\nu} \equiv G_{\mu,\nu} / L$ . With reference to Hamiltonian (1) it is natural to investigate the behavior of the fidelity under variations of the interaction parameter  $U$ . The possibility of analyzing variations of the chemical potential, though appealing does not fit in the fidelity approach as the ground states at different  $\mu$  belong to different superselection sectors. Hence now on we will solely be interested in  $g_{U,U}$  and we will simply write  $g$  in place of  $g_{U,U}$ . In Ref. 16 it was shown that it can be written in the following form:

$$g = \frac{1}{L} \sum_{n>0} \frac{|V_{n,0}|^2}{(E_n - E_0)^2}, \quad V = \sum_i n_{i,\uparrow} n_{i,\downarrow}, \quad (2)$$

where  $E_n, |n\rangle$  are the eigenenergies and corresponding eigenstates of the Hamiltonian (1) (with repulsion  $U$  and filling  $n$ ),  $|0\rangle$  corresponds then to the ground state and  $V_{i,j} = \langle i | V | j \rangle$ . In passing, we would like to notice that despite the apparent similarity between Eq. (2) and the second derivative of the energy  $E''(\lambda)$  (a similarity stressed in Ref. 24), it is possible to show—using the Rayleigh-Schrödinger series—that the metric tensor is in fact related to the third (and first) energy derivative via

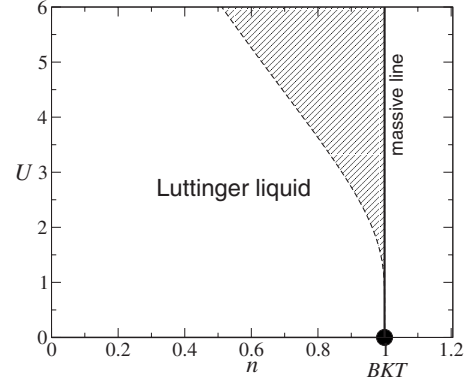


FIG. 1. Phase diagram of the repulsive Hubbard model. The region  $0 < n < 1$  is in the LL universality class. The hatched area corresponds to the condition  $\delta\xi(U) < 1$ , where  $\xi(U)$  is the correlation length at half-filling. Approaching the critical point ( $n=1, U=0$ ) from within (the complementary of) this region the LL parameter  $K_c$  approaches  $1/2$ , the BKT value (1, the free-Dirac value).

$$G = \frac{1}{V_{0,0} \sum_{i,j>0} (E_i - E_0)(E_j - E_0)} - \frac{E'''}{E'}.$$

Moreover, in the cases where  $E'''(\lambda)$  is bounded in the thermodynamic limit, one obtains the interesting kind of factorization relation  $\langle 0 | V | 0 \rangle \langle 0 | V \mathcal{G}(E_0)^2 V | 0 \rangle = \langle 0 | V \mathcal{G}(E_0) V \mathcal{G}(E_0) V | 0 \rangle$  valid in the thermodynamic limit, where  $\mathcal{G}$  is the resolvent  $\mathcal{G}(E) = (1 - |0\rangle\langle 0|)(H - E)^{-1} \times (1 - |0\rangle\langle 0|)$ .

In the rest of the paper we will be concerned with the analysis of the metric tensor with special care to the BKT transition point. The phase diagram of the Hubbard model is depicted in Fig. 1. The model has been solved by Bethe-Ansatz in Ref. 25. We will tackle the problem using a variety of techniques. On the free-gas  $U=0$  line, an explicit calculation is possible at all fillings. Around the region  $U=0$  and filling away from  $n=0$  and  $n=1$  bosonization results apply. Instead, close to the points  $U=0$  and  $n=1$  we will cross results from bosonization with Bethe-Ansatz in order to extend bosonization results up to the transition points. We will show that the behavior of the metric is encoded in a scaling function. Away from half-filling the scaling function is computed integrating Bethe-Ansatz equation, while at half-filling by resorting to exact diagonalization.

### III. EXACT ANALYSIS AT $U=0$

At  $U=0$  the complete set of eigenfunctions of Hamiltonian (1) is given by a filled Fermi sea and particle-hole excitations above it. It is then possible to apply directly Eq. (2).

#### A. Half-filling

We first treat the half-filled case  $n=1$ , where the Fermi momentum lies at  $k_F = \pi/2$ . Writing the interaction in Fourier space as  $V = L^{-1} \sum_{k,k',q} c_{k-k',\downarrow}^\dagger c_{k+q,\uparrow}^\dagger c_{k,\uparrow} c_{k',\downarrow}$  and going to the thermodynamic limit, Eq. (2) becomes

$$g = \frac{1}{(2\pi)^3} \int_{[-\pi, \pi]^3} \frac{n_k(1-n_{k+q})n_{k'}(1-n_{k'-q})}{(\epsilon_{k+q} - \epsilon_k + \epsilon_{k'-q} - \epsilon_{k'})^2} dk dk' dq, \quad (3)$$

where  $\epsilon_k = -2t \cos(k)$  is the  $U=0$  single-particle dispersion and  $n_k = \vartheta(-\epsilon_k)$  ( $=n_{k,\uparrow} = n_{k,\downarrow}$  in absence of magnetic field) are the fermionic zero-temperature filling factors. Using  $\epsilon(k, q) \equiv \epsilon_{k+q} - \epsilon_k = 4 \sin(q/2) \sin(k+q/2)$  and substituting  $k' \rightarrow -k'$  we obtain

$$g = \frac{1}{(2\pi)^3} \int_0^\pi dq \frac{1}{8 \sin(q/2)^2} \times \int_{-\pi}^\pi dk \int_{-\pi}^\pi dk' \frac{n(k, q)n(k', q)}{[\sin(k+q/2) + \sin(k'+q/2)]^2}.$$

Changing variables to  $p = k+q/2$  and  $p' = k'+q/2$  and making a shift of  $\pi/2$  we obtain finally

$$g = \frac{1}{(2\pi)^3} \int_0^\pi dq \frac{J(q)}{8 \sin(q/2)^2} = \frac{1}{24\pi^2} = 0.00422, \quad (4)$$

where we defined

$$J(q) = 4 \int_0^{q/2} dp \int_0^{q/2} dp' \frac{1}{[\cos(p) + \cos(p')]^2} \\ = -2 + 8 \frac{\ln[\cos(q/2)]}{\cos(q) - 1}$$

and correctly  $J(q) = J(-q) > 0$ .

A related interesting issue is that of the finite-size scaling of the metric tensor  $g$ , i.e., the way in which  $g_L$  at length  $L$  converges to its thermodynamic value (see also Ref. 6). In Ref. 17 it was shown that in a gapless regime scaling analysis predicts  $g_L \sim L^{-\Delta_g}$  apart from regular contributions which scale extensively (and contribute to  $g$  with a constant). Here  $\Delta_g = 2\Delta_V - 2\zeta - 1$ , where  $\Delta_V$  is the scaling dimension of  $V$  in the renormalization-group sense and  $\zeta$  is the dynamical critical exponent. On the line  $U=0$  one has  $\Delta_V = 2$  as  $V$  is a product of two independent free fields, while  $\zeta = 1$  when  $n \neq 0$  due to the linear dispersion of excitations at low momenta. This implies that at leading order  $g_L \sim A + BL^{-1}$ . One should however be careful that logarithmic corrections are not captured by the scaling analysis in Ref. 17 and they might be present due to the BKT transition occurring at this point. Let us try to clarify this issue. Looking at Eq. (4), as a first approximation, we might think that the finite size  $g_L$  is well approximated by the Riemann sum of  $F(q) \equiv J(q)/\sin(q/2)^2$ ,

$$g_L \approx \frac{S_L}{(2\pi)^3 8}, \quad S_L = \frac{2\pi}{L} \sum_{n=1}^{L/2} F\left(\frac{2\pi}{L} n\right).$$

Now  $F(q)$  diverges logarithmically around  $\pi^-$ :  $F(q) = -4 \ln(\frac{\pi-q}{2}) + O[(\pi-q)^2]$ , and since the Riemann sum of the logarithm converges to its integral as  $(A+B \ln L)/L + O(L^{-2})$  we would conclude

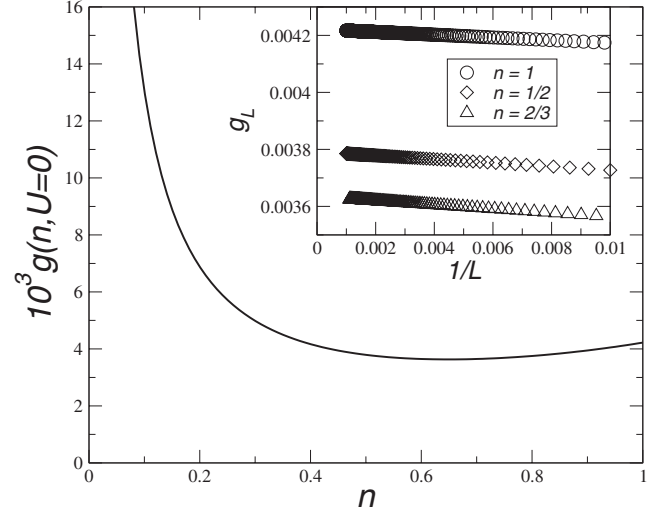


FIG. 2. Fidelity metric  $g$  as a function of the total density at  $U=0$ . The singularity at  $n \rightarrow 0$  is of the form  $n^{-1}$ . In the inset the finite-size scaling of  $g_L$  for some different fillings is shown. The approach to the thermodynamic value is given by Eq. (5) with  $B=0$ . In fact fitting the data points with Eq. (5) gives values of  $B/A$  of the order of  $10^{-4}$  and a  $\chi^2$  of the same order as the one obtained with  $B=0$ .

$$g_L - \frac{1}{24\pi^2} = \frac{A + B \ln L}{L} + \frac{C}{L^2} + O(L^{-4}). \quad (5)$$

However, a detailed analysis of the finite size  $g_L$  reveals that a *cancellation* occurs between two logarithmic corrections so that actually  $B=0$  in Eq. (5). The exact finite size  $g_L$  is composed of two terms. One term is a triple sum which, in the thermodynamic limit, corresponds to the triple integral in Eq. (3). The other term is a double sum which originates from zero transferred momentum contribution and vanishes when  $L \rightarrow \infty$ . We numerically verified that both terms contain a  $\ln L/L$  part when  $L \rightarrow \infty$ , but their contribution is equal and opposite so as to cancel out exactly from  $g_L$ . The absence of logarithmic corrections can clearly be seen in the inset of Fig. 2 where the finite size  $g_L$  is plotted against  $1/L$ .

### B. Away from half-filling

Similar considerations can be done away from half-filling. Equation (3) still holds simply in this case  $k_F \neq \pi/2$ . We assume  $k_F = n\pi/2 < \pi/2$  [anyway a particle-hole transformation implies  $g(n) = g(2-n)$ ]. First note that the integral over  $q$  can be recast as  $2 \int_0^\pi dq$ . The filling factors constrain the momenta to  $|k| < k_F$  and  $|k+q| > k_F$ . If  $q < 2k_F$  this implies  $k_F - q < k < k_F$ . Instead if  $q > 2k_F$  the sum over  $k$  is unconstrained:  $-k_F < k < k_F$ . Thus we obtain

$$g = \frac{2}{(2\pi)^3} \left\{ \int_0^{2k_F} dq \int_{k_F-q}^{k_F} dk \int_{k_F-q}^{k_F} dk' \right. \\ \left. + \int_{2k_F}^\pi dq \int_{-k_F}^{k_F} dk \int_{-k_F}^{k_F} dk' \right\} \\ \times \frac{1}{16 \sin(q/2)^2 [\sin(k+q/2) + \sin(k'+q/2)]^2}.$$

Changing variables as before and defining

$$J(a,b) \equiv \int_a^b dp \int_a^b dp' \frac{1}{[\sin(p) + \sin(p')]^2},$$

we obtain

$$g = \frac{1}{64\pi^3} \left\{ \int_0^{2k_F} dq \frac{J(k_F - q/2, k_F + q/2)}{\sin(q/2)^2} + \int_{2k_F}^{\pi} dq \frac{J(-k_F + q/2, k_F + q/2)}{\sin(q/2)^2} \right\}.$$

In Fig. 2 one can see a plot of  $g(n, U=0)$  as a function of the total density  $n = N_{\text{tot}}/L = 2k_F/\pi$ . It is possible to show that in the very dilute regime  $n \rightarrow 0$ , the fidelity metric  $g$  diverges in a simple algebraic way,

$$g(n \rightarrow 0, U=0) \sim \frac{1}{n}.$$

This divergence can also be simply understood by resorting to the scaling arguments reported in Ref. 17. There it was shown that in the thermodynamic limit  $g \sim |\mu - \mu_c|^{\Delta_g/\Delta_\mu}$ , where now  $\Delta_\mu$  is the scaling dimension of the field  $\mu$ . On the line  $U=0$  as already noticed  $\Delta_\nu=2$  while now  $\zeta=2$  as  $n \rightarrow 0$  to account for the parabolic dispersion. The chemical-potential scaling exponent is  $\Delta_\mu=2$  in the dilute Fermi gas.<sup>26</sup> All in all we obtain  $g \sim |\mu - \mu_c|^{-1/2} \sim n^{-1}$  since  $n \sim |\mu - \mu_c|^{1/2}$  which agrees with the explicit calculation.

The finite-size scaling of  $g_L$  for different fillings  $0 < n < 1$  is the same as that observed at  $n=1$  and is dictated by Eq. (5) with  $B=0$ , as can be seen in the inset of Fig. 2. Finally note that, since  $g(n, U=0)$  is symmetric around  $n=1$ ,  $g(n)$  has a local maximum at that point with a cusp. The origin of this discontinuity is not well understood at the moment but reveals a signature of the transition occurring at this point.

#### IV. BOSONIZATION APPROACH

It is well known<sup>20,21,27</sup> that for  $U \geq 0$  and away from half-filling ( $n=1$ ), the low-energy large distance behavior of the Hubbard model, up to irrelevant operators, is described by the Hamiltonian

$$H = H_s + H_c,$$

$$H_\nu = \frac{v_\nu}{2} \int d^2x \left[ K_\nu \Pi_\nu(x)^2 + \frac{1}{K_\nu} (\partial_x \Phi_\nu)^2 \right], \quad \nu = s, c. \quad (6)$$

Charge and spin degrees of freedom factorize and are described, respectively, by  $H_c$  and  $H_s$ . The Luttinger liquid parameters  $K_{c,s}$  are related to the long-distance algebraic decay of correlation functions, while  $v_{c,s}$  are the speed of elementary (gapless) charge and spin excitations. From bosonization and setting the lattice constant  $a=1$ , one finds, for small  $U$ ,

$$K_c = 1 - \frac{U}{2\pi v_F} + \dots, \quad (7)$$

where the Fermi velocity is  $v_F = 2t \sin(k_F)$  and  $k_F = \pi n/2$ . Instead the Luttinger parameter  $K_s$  is fixed to  $K_s=1$  due to

spin rotation invariance. Exactly at  $n=1$  there appears another term (an Umklapp term) in the charge sector which is marginally relevant and is responsible for the opening of a mass gap. In this case the effective theory is the sine-Gordon model.

Since the fidelity of two independent theories factorizes the metric tensor  $g$  is additive and we obtain  $g = g_s + g_c$ . In Ref. 15 the fidelity metric of a free boson theory has been calculated to be given by

$$g_\nu = \frac{1}{8} \left( \frac{1}{K_\nu} \frac{dK_\nu}{dU} \right)^2. \quad (8)$$

In our case  $g_s=0$  as  $K_s$  does not vary so that  $g = g_c + g_s = g_c$ . Using Eq. (7) one obtains a formula valid up to zeroth order in  $U$ ,

$$g = \frac{1}{2(4\pi v_F)^2} + O(U). \quad (9)$$

Some comments are in order. Expansion (7) is actually an expansion around  $U=0$  valid when  $U \ll v_F$ . When we move toward the BKT critical point one has  $v_F \rightarrow 2$  and  $g \rightarrow 1/(128\pi^2)$ . This value is  $3/16$  the number calculated directly at  $U=0$  in Sec. III A. We believe that this discrepancy is due to lattice corrections which are neglected in formula (8). Approaching the low-density critical point  $U=0$ ,  $n=0$  Eq. (9) predicts that, in a narrow region  $U \ll n$ , the fidelity metric diverges as  $g \sim n^{-2}$ . This contrasts with the result  $g \sim n^{-1}$  obtained at  $U=0$ , as one would expect since  $U$  is a relevant perturbation. In fact, in the diluted regime, the low-energy effective theory is that of a spinful nonrelativistic gas with delta interactions.<sup>20</sup> There one still has  $n \sim |\mu - \mu_c|^{1/2}$  and dynamical exponent  $\zeta=2$ . Thus if we take  $\Delta_\mu=1$ , then using the conventional scaling analysis we would find  $g \sim n^{-2}$ , consistent with the bosonization result.

#### V. HYPERSCALING OF FIDELITY METRIC NEAR THE METAL-INSULATOR CRITICAL POINT

The bosonization expression [Eq. (7)] is an expansion of  $K_c(n, U)$  around  $U=0$ , where  $K_c$  reaches its free-Dirac value of 1. In the whole stripe  $U \geq 0$ ,  $0 \leq n \leq 1$ ,  $K_c(n, U)$  is a bounded function ranging between  $1/2$  and  $1$ .<sup>28</sup> The maximal value  $K_c=1$  is obtained in the segment  $U=0$ . Instead the minimal value  $K_c=1/2$  is attained at the lines  $n=0$  and  $n=1$  and in the strong-coupling limit, i.e.,  $K_c \rightarrow 1/2$  for  $U \gg |t|$ . This considerations show that, from Eq. (8),  $g$  can be infinite only at the points  $U=0$  and  $n=0$  or  $1$ , where  $K_c$  is discontinuous. In particular, we are interested to the vicinity of the transition point  $U=0$ ,  $n=1$  which we will call simply (with some abuse) BKT point. Calling  $\xi(U)$  the correlation length at half-filling and  $\delta=1-n$  the doping concentration, it can be shown (see later) that the Luttinger liquid parameter  $K_c$  tends to  $1/2$  when the BKT point is approached from the region  $\delta\xi(U) \ll 1$ . Instead  $K_c \rightarrow 1$  when the BKT point is approached from  $\delta\xi(U) \gg 1$ . Given this discontinuity of  $K_c$  it seems difficult to interpolate between the two regimes  $\delta\xi(U) \ll 1$  and  $\delta\xi(U) \gg 1$ . However we will show that such an interpolation is indeed possible and that the fidelity metric



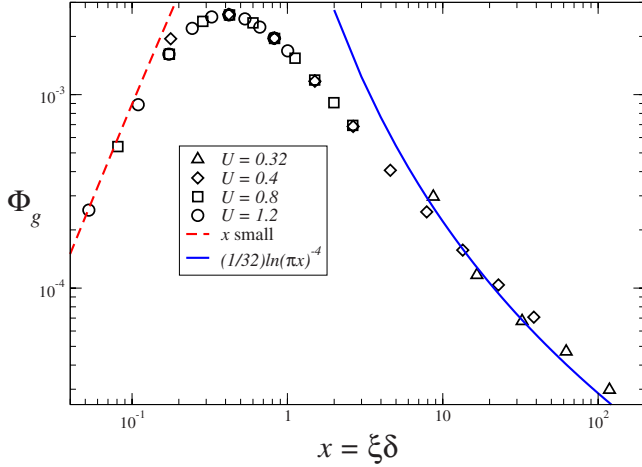


FIG. 3. (Color online) Scaling function  $\Phi_g$  for the fidelity metric as a function of the scaling parameter  $\xi\delta$ . Data are obtained by solving numerically the integral equations for the dressed charge at different interaction strengths  $U$ . The dashed line is obtained expanding the Bethe-Ansatz equations for the Luttinger parameter in the regime  $\xi\delta \ll 1$  up to second order in  $\delta$ . The solid line results from integrating the RG BKT equations and is valid when  $\xi\delta \gg 1$ .

$g$  satisfies an hyperscaling relation valid when  $\delta\xi$  ranges over many order of magnitudes (see Fig. 3).

In Refs. 29 and 30 an efficient characterization of the Luttinger liquid parameter  $K_c$  in terms of Bethe-Ansatz results has been found.  $K_c$  is related to the so-called dressed charge function  $Z_k$  through

$$K_c = Z_Q^2/2, \quad (10)$$

where the wave vector  $Q$  is a generalization of the Fermi wave vector in the interacting regime and has to be determined by Bethe-Ansatz equations. We will now argue that, in the metallic phase, the dressed charge function  $Z_Q$  satisfies the following scaling relation:

$$Z_Q(U, \delta) = \Phi_Z(\xi(U)\delta). \quad (11)$$

Here  $\xi(U)$  is the correlation length at half-filling ( $\delta=0$ ) defined via  $\xi = v_c/\Delta E_c$ , where  $v_c$  is the charge carries (holons) velocity and  $\Delta E_c$  is the (charge) gap, and  $\Phi_Z$  is a scaling function. Obviously a similar scaling relation holds for the Luttinger parameter  $K_c$  through Eq. (10). The scaling relation holds as long as the interaction is not too strong, say,  $U \leq 1$ . A similar scaling relation has been conjectured in Ref. 31 for the charge stiffness.

Using Eq. (8) we obtain the following scaling relation for the fidelity metric of the Hubbard model in the metallic phase close to the BKT point:

$$g(U, \delta) = \left( \frac{d \ln \xi}{dU} \right)^2 \Phi_g(\xi\delta), \quad (12)$$

where we introduced the scaling function  $\Phi_g(x) = (1/2)[x\Phi'_Z(x)/\Phi_Z(x)]^2$ . Following Ref. 31 it is natural to conjecture a more general hyperscaling relation for the fidelity metric valid also at finite size. Building the other dimen-

sionless quantity with the correlation length  $\xi$  and the size  $L$ , we obtain

$$g(U, \delta, L) = \left( \frac{d \ln \xi}{dU} \right)^2 Y(\xi\delta, \xi/L). \quad (13)$$

We will now verify the hyperscaling relation Eq. (13) away from half-filling in the thermodynamic limit ( $\xi/L=0$ ) using various analytical techniques and at finite size resorting to exact Lanczos diagonalization.

### A. Away from half-filling

The scaling relation Eq. (12) [and implicitly Eq. (11)] can be verified analytically in the two limits  $x = \xi\delta \rightarrow 0$  and  $x \rightarrow \infty$ . We present the results in terms of the Luttinger parameter  $K_c$  which has more physical relevance. In Refs. 30 and 32, the Bethe-Ansatz equations for the dressed charge have been solved around  $\delta=0$ . At leading order in  $\delta$ , they found for the Luttinger parameter,

$$K_c = \frac{1}{2} + a(U)\delta + \frac{1}{2}[a(U)\delta]^2 + O(\delta^3). \quad (14)$$

The function  $a(U)$  is studied in the Appendix and is approximately given by the following expansion for  $U/2\pi \ll 1$ :

$$a(U) \approx \frac{\ln(2)}{\sqrt{U}} e^{2\pi U}.$$

Not surprisingly, this has the same form as the soliton length,  $\xi(U)$ . In fact, for the regime of interest,  $U/2\pi \lesssim 1$ ,  $v_c \rightarrow 2$ , and  $\xi(U) = \pi a(U)/2 \ln(2)$ .<sup>31</sup> This implies that in the region  $x \ll 1$ , the metric scaling function behaves, at leading order, as

$$\Phi_g(x) = \left( \frac{\ln 4}{\sqrt{2\pi}} x \right)^2 + O(x^3).$$

Conversely, in the opposite regime  $\xi\delta \gg 1$  (i.e.,  $U \rightarrow 0$ ,  $\delta$  small) integrating the renormalization-group BKT equations,<sup>33</sup> one is able to improve the bosonization result Eq. (7) and we obtain

$$K_c = 1 - \frac{U/(4\pi)}{1 - U/(2\pi)\ln(1/\pi\delta)} = 1 - \frac{1}{2}[\ln(\pi\xi\delta)]^{-1} + \dots$$

Accordingly, the scaling function  $\Phi_g(x)$  has the following asymptotic behavior when  $x \rightarrow \infty$ :

$$\Phi_g(x) \approx \frac{1}{32}[\ln(\pi x)]^{-4}.$$

In the limit  $U \rightarrow 0$  we recover bosonization's result  $g \rightarrow 1/128\pi^2$ .

To verify the scaling relation [Eq. (12)] also in the intermediate regime  $\xi\delta \approx 1$ , we solved numerically the Bethe-Ansatz equations for the dressed charge.<sup>20</sup> To obtain the dressed charge function  $Z_k$  we need also the density of wave numbers  $\rho_k$ . They are solutions of the following integral equations:

$$\rho_k = 1 - \cos(k) \int_{-Q}^Q dq \cos q R(\sin k - \sin q) \rho_q, \quad (15)$$

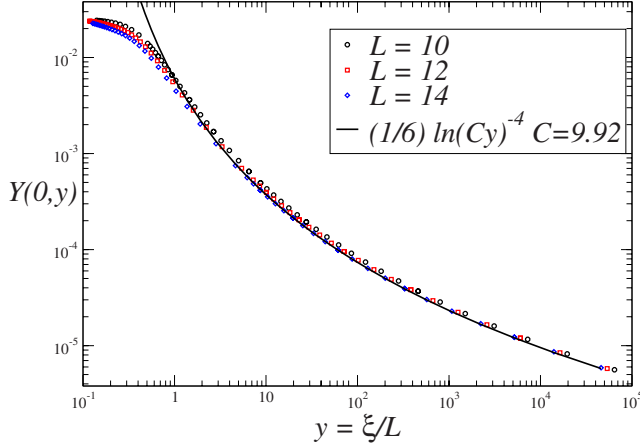


FIG. 4. (Color online) Finite-size scaling function  $Y(0, y)$  as a function of the normalized correlation length  $\xi/L$ . The solid line was obtained by requiring consistency with the noninteracting value at  $U=0$ . The constant  $C$  is obtained by a best fit with the numerical data (symbols). Boundary conditions are antiperiodic when system size  $L$  is a multiple of four periodic otherwise.

$$Z_k = 1 + \int_{-Q}^Q dq \cos qR(\sin k - \sin q)Z_q, \quad (16)$$

with  $R(x)$  given by

$$R(x) = \frac{1}{2\pi} \int_{-\infty}^{\infty} d\omega \frac{e^{i\omega x}}{1 + e^{U|\omega|/2}}.$$

The wave vector  $Q$  is determined by fixing the electronic density  $n = \int_{-Q}^Q \rho_k dk$ . Integrating numerically Eqs. (15) and (16) for different values of the coupling strength and doping fraction, we are able to verify the scaling relation [Eq. (12)] over many orders of magnitude. The result is plotted in Fig. 3.

We would like to point out that since close to the BKT point the relevant variable is  $\xi(U)\delta$ , the limit of the fidelity metric when  $U \rightarrow 0$  and  $n \rightarrow 1$  depends on the path of approach. However, as we have shown, the combination  $g(d \ln \xi/dU)^{-2}$  is a perfectly well defined function of  $\xi\delta$ .

### B. Numerical analysis at half-filling

To study the scaling behavior of the metric at half-filling, we turned to exact Lanczos diagonalization. We find that the metric obeys the scaling form Eq. (13) with the scaling function  $Y(0, y)$  plotted in Fig. 4 for values of its argument ranging over six orders of magnitude.

After calculating the ground state  $\Psi_0(U)$  of Hamiltonian (1) with the Lanczos algorithm, the intensive fidelity metric  $g$  is obtained from the fidelity  $F(U, U + \delta U) = |\langle \Psi_0(U) | \Psi_0(U + \delta U) \rangle|$  using

$$g_L = \frac{2}{L} \frac{1 - F(U, U + \delta U)}{\delta U^2}, \quad (17)$$

with  $\delta U = 10^{-3}$ . The above equation is a good approximation to the limit  $\delta U \rightarrow 0$  as long as  $\delta U \ll 1/\sqrt{Lg}$  which was confirmed to be the case in all simulations. The function  $Y(0, y)$

is then obtained via  $Y = g_L(d \ln \xi/dU)^{-2}$ . In order to have as many data points as possible, we analyzed sizes of length  $L=4n+2$  with periodic boundary conditions (BCs), while for length  $L=4n$  antiperiodic boundary conditions were used. Choosing such boundary conditions at half-filling assures that the ground state is nondegenerate even at  $U=0$ .<sup>34</sup>

The behavior at large  $y = \xi/L$  can be obtained by requiring consistency with the value obtained in the free case  $U=0$ . Then the scaling function must have the following limiting form:

$$Y(0, y) = \frac{1}{6} [\ln(Cy)]^{-4}, \quad y \rightarrow \infty,$$

where  $C$  is a constant. Since when  $y \rightarrow \infty$   $\ln \xi \sim 2\pi/U$  the divergence in  $(d \ln \xi/dU)^2$  cancels with the logarithm above, and one obtains

$$g(U \rightarrow 0, L) = \frac{1}{24\pi^2} \left( \frac{\ln(\xi)}{\ln(C\xi/L)} \right)^4 = \frac{1}{24\pi^2}.$$

Having computed the scaling function  $Y(x, y)$  we could ask what happens to the metric tensor as one approaches the BKT point from the particular path  $U \rightarrow 0, n=1$ . The smallest values of  $y$  at our disposal are of the order of  $y \sim 10^{-1}$ . Looking at Fig. 4, on the basis of these data, it seems that the function  $Y$  approaches a nonzero value  $\lim_{y \rightarrow 0} Y(0, y)$  as  $y$  goes to zero. If this is the case, after taking  $L \rightarrow \infty$  and  $U$  small we would have

$$\lim_{L \rightarrow \infty} g(U, n=1, L) = \frac{4\pi^2}{U^4} Y(0, 0).$$

Note however that observing this divergence numerically can be very hard as we must be in the region  $L \gg \xi(U)$  which requires huge sizes when the coupling  $U$  is small.

## VI. CONCLUSIONS

In this paper we analyzed the *fidelity metric* in the zero-temperature phase diagram of the 1D Hubbard model with particular care at the phase-transition points. The fidelity metric quantifies the degree of distinguishability between a state and its neighbors in the space of states, and as such it is expected to increase (or diverge) at transition points. Special attention has been drawn to assess whether the fidelity metric reveals signatures of the Mott-insulator transition occurring at on-site repulsion  $U \rightarrow 0$  and filling factor  $n=1$ . Being a transition of infinite order, it is particularly difficult to pin down since typical thermodynamic quantities are smooth (although not analytic) at the transition. The point  $U=0, n=1$  is particularly singular in that it represents the limit of two completely different physical regimes. On the line  $U=0$  it is simply the half-filling limit of a gapless free system, whereas fixing  $n=1$  it represents the limit of a complicated interacting massive system. Surprisingly, we have shown that it is possible to interpolate between these two regimes, and the fidelity metric defines a hyperscaling function which depends only on  $x = \xi(U)(1-n)$ . The two regimes roughly correspond to  $x \gg 1$  and  $x \ll 1$ , respectively.

Away from half-filling we have been able to compute the scaling function integrating numerically Bethe-Ansatz equa-

tions, and we obtained analytic expressions for the limits  $x \rightarrow 0, \infty$ . The result implies that, as a function of  $U$  and  $n$  separately, the fidelity metric has no precise limit when  $U \rightarrow 0, n \rightarrow 1$ , but the scaling function is well defined in term of the scaling variable  $x$ .

Precisely at half-filling we computed the scaling function resorting to exact diagonalization and upon introduction of another scaling variable  $y = \xi(U)/L$ . With the numerical data at our disposal, the scaling function appears to be smooth and nonzero around  $y=0$ . As a consequence, approaching the Mott point from the half-filling line, the fidelity metric would display a singularity of the form  $U^{-4}$ . A singularity of algebraic type has been observed also in another instance of Kosterlitz-Thouless transition given by the XXZ model.

#### ACKNOWLEDGMENTS

L.C.V. would like to thank Cristian Degli Esposti Boschi for a critical reading of the manuscript. P.B. acknowledges financial support from the PRIN project *Microscopic description of fermionic quantum devices* as well as from the CNISM project *Quantum Phase Transitions, Nonlocal Quantum Correlations, and Nonlinear Dynamics in Ultracold Lattice Boson Systems*.

#### APPENDIX

Following Ref. 30 the coefficient  $a$  in Eq. (14) is given by

$$a(U) = \frac{4 \ln(2)}{U f(U)},$$

where

$$f(U) \equiv 1 - 2 \int_0^\infty \frac{J_0(x)}{1 + e^{Ux/2}} dx,$$

and  $J_0$  is a Bessel function. Using the following results:

$$\begin{aligned} \frac{1}{1 + e^{\alpha x}} &= \sum_{n=0}^{\infty} (-1)^n e^{-(n+1)\alpha x} \int_0^\infty J_0(x) e^{-\beta x} dx \\ &= \frac{1}{\sqrt{1 + \beta^2}}, \quad \alpha, \beta > 0, \end{aligned}$$

we arrive at

$$f(U) = 1 + 2 \sum_{n=1}^{\infty} (-1)^n \frac{1}{\sqrt{1 + n^2 U^2/4}}.$$

Using the formalism of the remnant functions defined in Ref. 35 one realizes that  $f(U)$  is related to  $R_{1/2,0}^{(-)}(4U^{-2})$ . With the help of the expansions in Ref. 35 we obtain the following expression:

$$f(U) = \frac{8}{U} \sum_{n=0}^{\infty} K_0 \left( \frac{2\pi}{U} (2n+1) \right).$$

It is now easy to obtain the desired expression using the asymptotic of the Bessel function,

$$K_0(1/x) = e^{-1/x} \sqrt{\frac{\pi x}{2}} \left( 1 - \frac{1}{8}x + \frac{9}{128}x^2 + O(x^3) \right).$$

Collecting the results together, we obtain at leading order

$$a(U) = \frac{\ln(2)}{\sqrt{U}} e^{2\pi/U} [1 + O(U)].$$

- 
- <sup>1</sup>P. Zanardi and N. Paunkovic, Phys. Rev. E **74**, 031123 (2006).  
<sup>2</sup>H. Q. Zhou and J. P. Barjaktarevic, arXiv:cond-mat/0701608 (unpublished).  
<sup>3</sup>P. Zanardi, M. Cozzini, and P. Giorda, J. Stat. Mech.: Theory Exp. 2007, L02002 (2007).  
<sup>4</sup>M. Cozzini, P. Giorda, and P. Zanardi, Phys. Rev. B **75**, 014439 (2007).  
<sup>5</sup>M. Cozzini, R. Ionicioiu, and P. Zanardi, Phys. Rev. B **76**, 104420 (2007).  
<sup>6</sup>W. L. You, Y. W. Li, and S. J. Gu, Phys. Rev. E **76**, 022101 (2007).  
<sup>7</sup>S. J. Gu, H. M. Kwok, W. Q. Ning, and H. Q. Lin, Phys. Rev. B **77**, 245109 (2008).  
<sup>8</sup>H. Q. Zhou, arXiv:0704.2945 (unpublished).  
<sup>9</sup>P. Buonsante and A. Vezzani, Phys. Rev. Lett. **98**, 110601 (2007).  
<sup>10</sup>A. Hamma, W. Zhang, S. Haas, and D. Lidar, Phys. Rev. B **77**, 155111 (2008).  
<sup>11</sup>H. Q. Zhou and B. L. J. H. Zhao, arXiv:0704.2940 (unpublished).  
<sup>12</sup>S. Chen, L. Wang, S. J. Gu, and Y. Wang, Phys. Rev. E **76**, 061108 (2007).  
<sup>13</sup>H. Q. Zhou, J. H. Zhao, H. L. Wang, and B. Li, arXiv:0711.4651 (unpublished).  
<sup>14</sup>S. L. Zhu, Phys. Rev. Lett. **96**, 077206 (2006).  
<sup>15</sup>M.-F. Yang, Phys. Rev. B **76**, 180403(R) (2007); note that recently the result of Yang for the fidelity metric has been corrected by a factor 1/2 (Ref. 36).  
<sup>16</sup>P. Zanardi, P. Giorda, and M. Cozzini, Phys. Rev. Lett. **99**, 100603 (2007).  
<sup>17</sup>L. Campos Venuti and P. Zanardi, Phys. Rev. Lett. **99**, 095701 (2007).  
<sup>18</sup>An almost standard route is that of adding an electric/magnetic field and to measure the corresponding stiffness which experiences a jump at the transition (see Ref. 37).  
<sup>19</sup>The term BKT is justified in the sense that the underlying effective theory is the sine-Gordon model (see later). In the condensed-matter literature the term Mott transition is more commonly used.  
<sup>20</sup>F. H. L. Essler, H. Frahm, F. Göhmann, A. Klümper, and V. E. Korepin, *The One-Dimensional Hubbard Model* (Cambridge University Press, Cambridge, 2005).  
<sup>21</sup>J. Sólyom, Adv. Phys. **28**, 201 (1979).  
<sup>22</sup>J. Voit, Rep. Prog. Phys. **58**, 977 (1995).

- <sup>23</sup>C. Itzykson and J.-M. Drouffe, *Statistical Field Theory* (Cambridge University Press, Cambridge, 1989).
- <sup>24</sup>S. Chen, L. Wang, Y. Hao, and Y. Wang, *Phys. Rev. A* **77**, 032111 (2008).
- <sup>25</sup>E. H. Lieb and F. Y. Wu, *Phys. Rev. Lett.* **20**, 1445 (1968).
- <sup>26</sup>S. Sachdev, *Quantum Phase Transitions* (Cambridge University Press, Cambridge, 1999).
- <sup>27</sup>V. J. Emery, *Highly Conducting One-Dimensional Solids* (Plenum, New York, 1979), p. 327.
- <sup>28</sup>H. J. Schulz, *Phys. Rev. Lett.* **64**, 2831 (1990).
- <sup>29</sup>N. Kawakami and S.-K. Yang, *Phys. Lett. A* **148**, 359 (1990).
- <sup>30</sup>H. Frahm and V. E. Korepin, *Phys. Rev. B* **42**, 10553 (1990).
- <sup>31</sup>C. A. Stafford and A. J. Millis, *Phys. Rev. B* **48**, 1409 (1993).
- <sup>32</sup>A. Schadschneider and J. Zittartz, *Z. Phys. B: Condens. Matter* **82**, 387 (1991).
- <sup>33</sup>E. B. Kolomeisky and J. Straley, *Rev. Mod. Phys.* **68**, 175 (1996).
- <sup>34</sup>Note also that both these classes of fermionic systems with different boundary conditions can be mapped onto an interacting systems of hard-core bosons with periodic boundary conditions. This clarifies further why it is possible to compare data obtained with different boundary conditions.
- <sup>35</sup>M. E. Fisher and M. N. Barber, *Arch. Ration. Mech. Anal.* **47**, 205 (1972).
- <sup>36</sup>J. O. Fjærestad, *J. Stat. Mech.: Theory Exp.* 2008, P07011 (2008).
- <sup>37</sup>N. Laflorencie, S. Capponi, and E. S. Sorensen, *Eur. Phys. J. B* **24**, 77 (2001).